Contents lists available at ScienceDirect

Journal of Biomechanics

journal homepage: www.elsevier.com/locate/jbiomech

Artificial intelligence-enhanced 3D gait analysis with a single consumer-grade camera

Ling Guo [a,b], Richard Chang [b], Jie Wang [a,b], Amudha Narayanan [b], Peisheng Qian [b], Mei Chee Leong [b], Partha Pratim Kundu [a,b], Sriram Senthilkumar [a], Sai Chaitanya Garlapati [a], Elson Ching Kiat Yong [a], Ramanpreet Singh Pahwa [a,b,*]

[a] Carecam Pte Ltd., Singapore
[b] Institute for Infocomm Research (I2R), Agency for Science, Technology and Research (A*STAR), Singapore

ARTICLE INFO

Keywords:
Gait analysis
Single-camera motion capture
Clinical gait assessment
Markerless motion capture
Deep learning

ABSTRACT

Gait analysis is crucial for diagnosing and monitoring various healthcare conditions, but traditional marker-based motion capture (MoCap) systems require expensive equipment, extensive setup, and trained personnel, limiting their accessibility in clinical and home settings. Markerless systems reduce setup complexity but often require multiple cameras, fixed calibration, and are not designed for widespread clinical adoption. This study introduces 3DGait, an artificial intelligence-enhanced markerless 3-Dimensional gait analysis system that operates with a single consumer-grade depth camera, providing a streamlined, accessible alternative. The system integrates advanced machine learning algorithms to produce 49 angular, spatial, and temporal gait biomarkers commonly used in mobility analysis. We validated 3DGait against a marker-based MoCap (OptiTrack) using 16 trials from 8 healthy adults performing the Timed Up and Go (TUG) test. The system achieved an overall average mean absolute error (MAE) of 2.3°, with all MAE under 5.2°, and a Pearson's correlation coefficient (PCC) of 0.75 for angular biomarkers. All spatiotemporal biomarkers had errors no greater than 15 %. Temporal biomarkers (excluding TUG time) had errors under 0.03 s, corresponding to one video frame at 30 frames per second. These results demonstrate that 3DGait provides clinically acceptable gait metrics relative to marker-based MoCap, while eliminating the need for markers, calibration, or fixed camera placement. 3DGait's accessible, non-invasive and single camera design makes it practical for use in non-specialist clinics and home settings, supporting patient monitoring and chronic disease management. Future research will focus on validating 3DGait with diverse populations, including individuals with gait abnormalities, to broaden its clinical applications.

1. Introduction

Gait analysis plays a critical role in healthcare by helping to diagnose, treat and monitor neurological disorders, musculoskeletal issues, and post-surgery recovery among others (Muro-de-la-Herran et al., 2014; Simon, 2004; Whittle, 2014). Traditionally, quantitative gait analysis relies on marker-based motion capture (MoCap) systems, which uses reflective markers and high-speed cameras to track movement with millimeter accuracy (Aurand et al., 2017; Ehara et al., 1997, 1995; Richards, 1999). However, these systems are expensive, cumbersome and time-consuming, requiring significant effort and expertise for meticulous marker placement and data processing (Hulleck et al., 2022; Scataglini et al., 2024; Scott et al., 2022; Simon, 2004). Additionally, the presence of markers and setup constraints can affect the naturalness of movement, introducing biases in analysis (Colyer et al., 2018; Moro et al., 2022; Scataglini et al., 2024). These challenges restrict their use in routine clinical practice and home monitoring.

Advances in sensors, signal processing and artificial intelligence (AI) have made quantitative gait analysis more accessible and scalable across research and clinical settings (Hulleck et al., 2022; Lam et al., 2023; Stenum et al., 2024). Wearables like inertial measurement units (IMUs) are portable and affordable (Homan et al., 2022; Liu et al., 2021; Saboor et al., 2020; Tadano et al., 2013) but suffer from sensor drift, placement sensitivity, and calibration requirements, limiting their usability (Hulleck et al., 2022; Liu et al., 2021; Muro-de-la-Herran et al., 2014). Pressure-sensitive gait mats provide reliable spatiotemporal gait

* Corresponding author at: 1 Fusionopolis Way, #21-01 Connexis, Singapore 138632, Singapore.
E-mail address: ramanpreet_pahwa@i2r.a-star.edu.sg (R.S. Pahwa).

https://doi.org/10.1016/j.jbiomech.2025.112738
Accepted 29 April 2025

parameters (Dogan et al., 2024; Webster et al., 2005) but lack joint angle measurements, portability, and real-world applicability (Muro-de-la-Herran et al., 2014; Saboor et al., 2020).

Markerless MoCap systems leverage AI and computer vision for gait analysis without body markers, reducing setup complexity and time (Corazza et al., 2006; Lam et al., 2023; Mündermann et al., 2006), and allowing for more natural movement (Colyer et al., 2018; Moro et al., 2022; Scataglini et al., 2024). They eliminate marker placement errors, improving repeatability across sessions, and automate data processing which enhances efficiency (Mathis et al., 2020; Wade et al., 2022). Some systems work with consumer-grade devices like smartphone cameras, increasing accessibility and adaptability to various environments (Drazan et al., 2021; Uhlrich et al., 2023).

Despite their advantages, markerless MoCap systems face limitations that hinder widespread clinical adoption (Hulleck et al., 2022). High accuracy systems like Theia3D are expensive, require multi-camera setups, complex software and calibration (Kanko et al., 2021a; Wren et al., 2023). Lower-cost multi-camera systems still require careful calibration and are designed for research use, requiring biomechanics expertise and lacking automatic generation of relevant clinical gait parameters (Drazan et al., 2021; Uhlrich et al., 2023; Wang et al., 2024). Broader clinical adoption requires integration into intuitive and user-friendly platforms (Lam et al., 2023).

Single-camera solutions are cost-effective and easy to use, but are less accurate than multi-camera setups (Boldo et al., 2024; Scott et al., 2022; Springer and Seligmann, 2016; Viswakumar et al., 2022; Wang et al., 2024). Many (Boldo et al., 2024; Moro et al., 2022; Stenum et al., 2021; Viswakumar et al., 2022) rely on generic, open-source pose estimation models like OpenPose (Cao et al., 2017), which are not optimized for biomechanics applications (Wade et al., 2022). These models often mislabel or fail to label joint centers, and compute only two points per body segment, insufficient for calculating six degrees of freedom needed for clinical gait analysis (Needham et al., 2021; Wade et al., 2022). Furthermore, they estimate 2D instead of 3D poses, assuming movements occur strictly in the frontal or sagittal plane, making accuracy heavily dependent on camera alignment (Wade et al., 2022). Occlusions and limited depth perception further impact the precision of spatial parameters and joint kinematics parallel to the camera's line of sight (Stenum et al., 2021; Wade et al., 2022).

To overcome these limitations, we developed 3DGait, an end-to-end gait analysis application that uses a single consumer-grade camera with depth sensor to generate 49 angular and spatiotemporal gait biomarkers. Unlike conventional single-camera systems, 3DGait employs biomechanically accurate key points, leverages advanced AI algorithms for full 3D pose estimation, and integrates depth sensing, to improve accuracy while reducing dependence on camera alignment. The system is fully automated, and wearable-independent, making it practical for clinics, homes, and everyday environments. In this study, we validate 3DGait by comparing its gait measurements in healthy adults against marker-based MoCap, demonstrating its accuracy and usability. A more detailed comparison with existing markerless solutions is provided in the Discussion section.

2. Methods

2.1. 3DGait system architecture

3DGait consists of modules (Fig. 1, Table 1) that process video and Light Detection And Ranging (LiDAR) data of a subject performing a Timed Up and Go (TUG) test or a back-and-forth walk, captured using an iPad Pro (2nd generation and above, Apple Inc., CA, USA). The system detects and tracks the Person of Interest (PoI), extracts 2D key points (Fig. 2), and converts them into 3D pose estimates. Smoothing, scaling, and translation refine these estimates using LiDAR data for real-world alignment. Phase segmentation and gait segmentation identify movement phases and gait events, while ground plane estimation provides spatial reference. Finally, gait parameter computation derives angular kinematics and spatiotemporal biomarkers. All processing occurs locally on the iPad, with automatic face blurring and an option to delete video files immediately. The recommended working conditions of 3DGait are described in Sup. Table S1. 3DGait's user-friendly interface also provides real-time guidance on camera and subject placement to facilitate optimal data collection (Sup. Fig. S1).

2.2. Participants and dataset description

Data from 72 healthy adults were collected for development and evaluation of 3DGait. The study was deemed Institutional Review Board

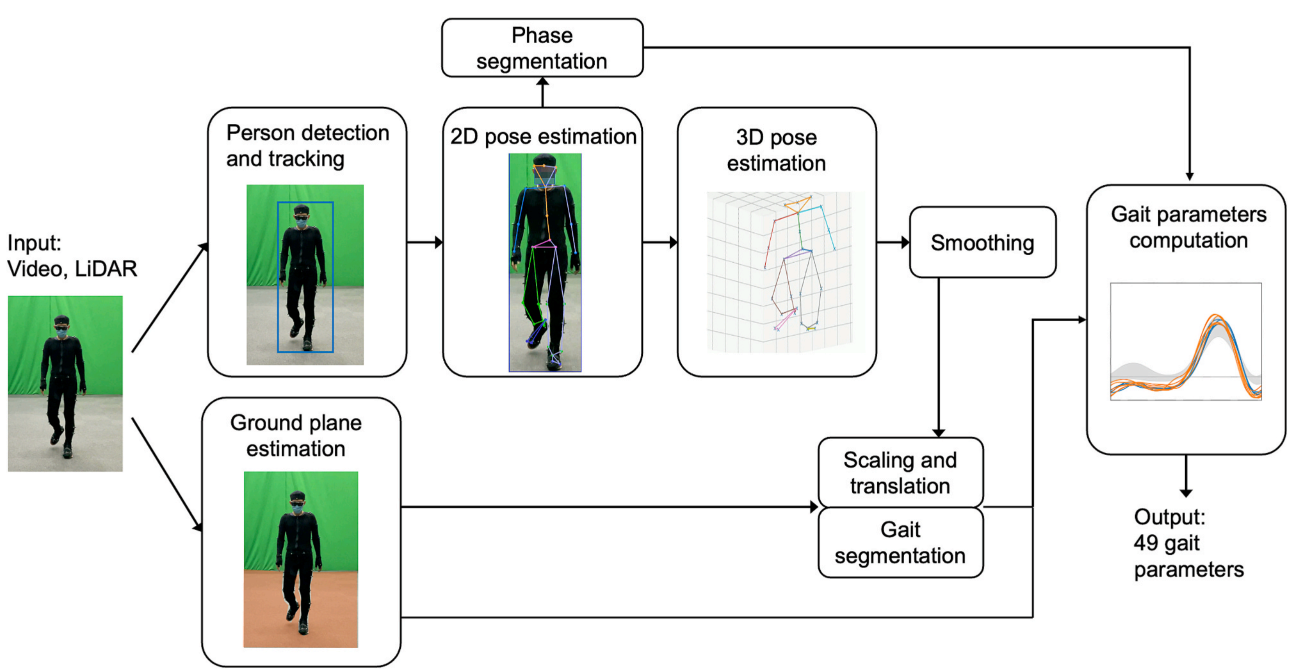

Fig. 1. Architecture of 3DGait.

Table 1
Description of modules within 3DGait.

Module	Function	Methods/techniques used	Output
Person Detection and Tracking	Detects and tracks individuals in the video	You Only Look Once (YOLO) model(Wang et al., 2023) pretrained on the Microsoft Common Objects in Context (MS-COCO) dataset (Lin et al., 2014), deepSORT (Wojke et al., 2017)	Person of Interest (PoI) performing the task identified in video frames
2D Pose Estimation	Computes 2D body key points	Lightweight Pose Network (Sun et al., 2019; Xiao et al., 2018, Zhang et al., 2019)	[x, y] coordinates of 28 keypoints (Fig. 2), adapted from CAST marker set (Cappozzo et al., 1995)
3D Pose Estimation	Transforms 2D body key points into 3D	Videopose3D (Pavllo et al., 2019)	Normalized [x, y, z] coordinates of 28 body key points
Smoothing	Reduces noise in 3D pose	4th order 6 Hz low-pass Butterworth filter(Winter, 2009)	Smoothed 3D coordinates
Scaling and Translation	Converts normalized 3D poses to real-world dimentions	LiDAR-based scaling and translation	Real-world [x, y, z] coordinates of key points
Phase Segmentation	Identifies movement phases (sit, stand, walk, turn)	Object detection and 2D pose-based algorithmic segmentation	Frame numbers marking phase transitions
Ground Plane Estimation	Estimates ground plane for gait segmentation and biomarker computation	LiDAR data and *ransac* algorithm (Fischler and Bolles, 1981)	Ground plane parameters
Gait Segmentation	Determines gait phases (swing, stance)	Algorithmic approach using 3D foot key points and ground plane	Gait cycle time events
Gait Parameters Computation	Computes joint angles and gait parameters	Joint Coordinate System framework (Grood and Suntay, 1983) for joint kinematics, timing of gait events and 3D keypoints for spatiotemporal gait parameters	Angular joint kinematics, spatiotemporal gait parameters

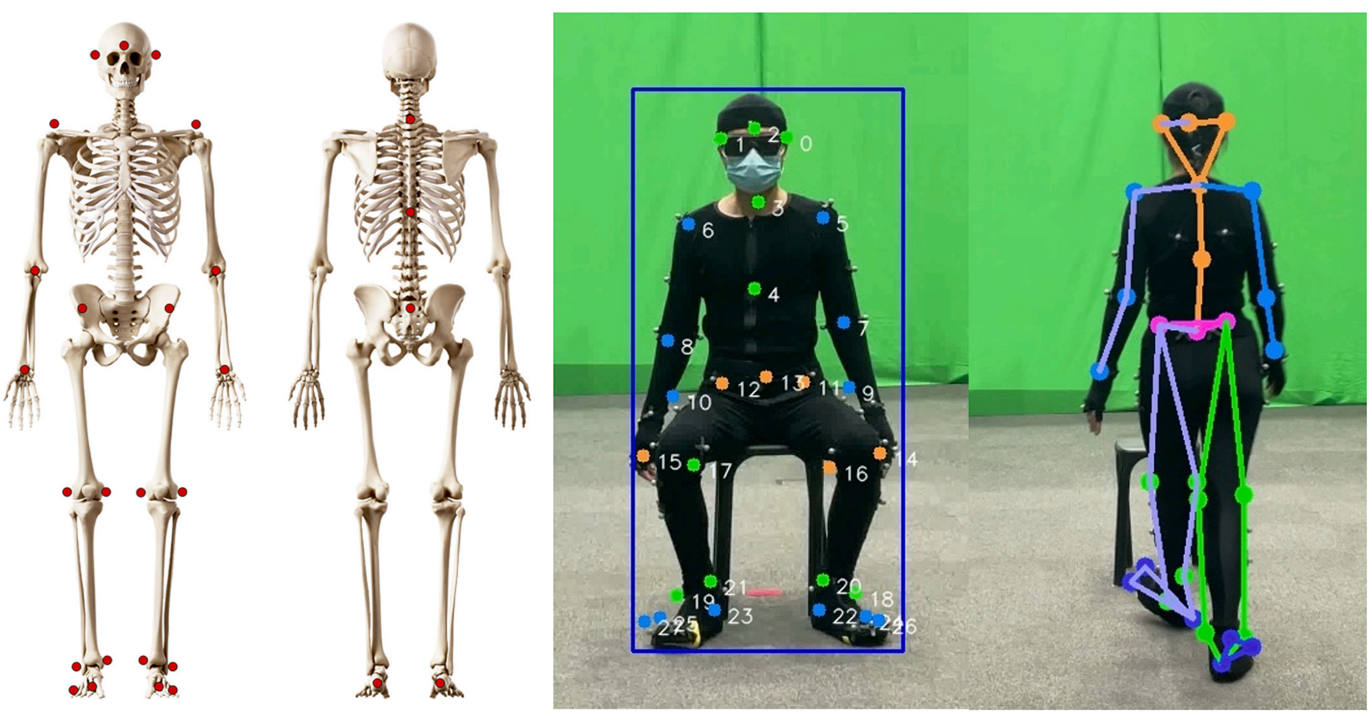

Fig. 2. The positions of the 28 key points used by the proposed 3DGait algorithm, drawn on a skeleton (left) and project on an example subject (right).

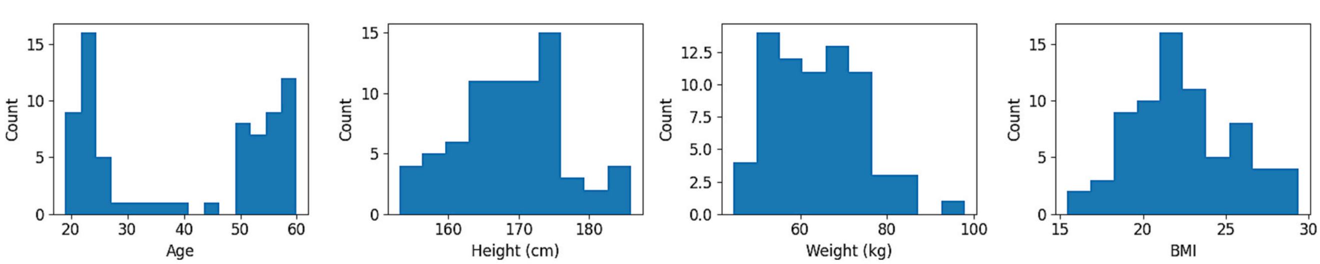

Fig. 3. The age, height, weight and body mass index (BMI) distributions of subjects.

(IRB) exempt by the Agency for Science, Technology and Research (A*STAR), Singapore (IRB 2023–040), because the data collection was observational and de-identified. Subjects were recruited in four equal demographic groups: males under 50 (n = 18), males 50+ (n = 17), females under 50 (n = 18), and females 50+ (n = 19). Exclusion criteria included mobility issues or difficulty walking with a mask and sunglasses. The age, height, weight and body mass index (BMI) distributions of the subjects are shown in Fig. 3. Data collection took place in a motion capture studio in Beijing, China, by Datatang, a contracted company, with all subjects of Chinese ethnicity.

The dataset was divided into training, used to develop the 2D and 3D pose estimation models, and testing sets, used for system evaluation. The test set included the first 8 subjects (4 males, 4 females, mean age 44.8, standard deviation (SD) 13.2, 16 trials total), with complete data who successfully completed the 6 m TUG. The training dataset comprised 31 males, 33 females (mean age 39.5, SD 16.3).

2.3. Experimental set up and procedures

Color videos and LiDAR data were acquired simultaneously using 4 iPad Pro (Apple Inc., CA, USA) at 30 frames per second (FPS). Cameras were placed to ensure full subject visibility throughout the trial. While multiple camera angles were recorded for training, 3DGait processes only the front-facing camera, which was positioned approximately 3.5 m from the end of the walkway (Sup. Fig. S2). All cameras were placed at a height of 1.2–1.6 m from the ground. Data was acquired with consistent overhead ambient lighting in a controlled indoor environment (see Fig. 2 and Sup. Fig. S3a for examples).

Motion data was concurrently captured using the OptiTrack system (NaturalPoint Inc., OR, USA) with 60 OptiTrack Prime 41 cameras at 120 Hz. Markers were placed according to the CAST marker set (Cappozzo et al., 1995). Subjects performed several trials of 3 m and 6 m TUG tests, and a 6 m back and forth walk, once in a black body suit with reflective markers for ground truth MoCap data collection and once in regular clothing (see Sup. Fig. S3a for examples) to ensure model performance under real-world conditions. MoCap data was manually inspected, and trials with missing or misplaced markers were excluded.

2.4. Pose estimation model training

The 2D pose model was trained using images extracted from iPad videos, with 2D key points reprojected from MoCap 3D data or manually annotated. The dataset included diverse lighting conditions, clothing, backgrounds, and camera angles, supplemented with images from open environments and MS-COCO (Lin et al., 2014). The 3D model was trained using paired 2D-3D coordinates from MoCap. Training data was augmented to include variations in camera angles and subject locations to improve generalizability. The hyperparameters of both models are summarized in Sup. Table S2. These were selected based on prior work, specifically the Lightweight Pose Network (LPN) (Sun et al., 2019; Xiao et al., 2018; Zhang et al., 2019) for 2D pose and VideoPose3D (Pavllo et al., 2019) for 3D pose, or performance on a held-out subset of the training data. Batch sizes were selected to optimize for training speed given available computational resources. Both models were converted to TensorFlow Lite for efficient edge computing.

2.5. System evaluation

The 2D pose model was evaluated on test subjects wearing black bodysuits and everyday clothing, and on the MS-COCO validation set (Sup. Fig. S3), using Object Keypoint Similarity (OKS) (Maji et al., 2022) and pixel distance error. OKS, ranging 0–1 measures normalized keypoint overlap—higher is better—while pixel error captures absolute point deviations in pixels—lower is better. The 3D pose estimation model was evaluated using the Mean Per-Joint Position Error (MPJPE) in millimeters, the average Euclidean distances between predicted and ground truth 3D positions, with lower MPJPE indicating higher accuracy.

To evaluate the final gait parameters, ground truth joint kinematics were computed from the 3D MoCap data using the Joint Coordinate System (Grood and Suntay, 1983). The ground truth temporal biomarkers were based on manual video annotation, while spatial biomarkers were based on annotated time boundaries and 3D coordinates. The accuracy of angular biomarkers was measured using mean-shifted Mean Absolute Error (MAE) in degrees and Pearson's Correlation Coefficient (PCC) between the 3DGait and ground truth values. The mean-shifted MAE is calculated by first subtracting the average angle value across the gait cycle, which reduces variability due to marker placement inconsistencies, as described in Wren et al. (2023). The spatiotemporal biomarkers were evaluated using MAE in seconds, meters and meters per second, with errors also expressed as percentages of ground truth value.

2.6. Statistical analysis

All analyses were conducted in Python (v3.9) using SciPy, NumPy and spm1d. Joint kinematics and spatiotemporal biomarkers were averaged across gait cycles within trials and then across all test subjects. 95 % confidence intervals were computed using the t-distribution due to the small sample size. A paired *t*-test was performed on the joint kinematics using Statistical Parametric Mapping (SPM1d), which applies random field theory to adjust for multiple comparisons. Regions where t-values exceeded the critical threshold ($p < 0.05$) were identified as significantly different between 3DGait and MoCap measurements.

3. Results

3.1. Performance of pose estimation models

Table 2 summarizes model performance for the 2D and 3D pose models in 3DGait. When tested on subjects in everyday clothing (Sup. Fig. S3a), OKS was 0.875—only a 1.6 % decrease compared to those in black body suits (OKS of 0.889). On the more challenging MS-COCO dataset (Sup. Fig. S3b), OKS was 0.835, reflecting a 6 % reduction. To further illustrate robustness, we overlaid inferred 2D key points on images acquired in diverse environments with different clothing and lighting conditions (Sup. Fig. S3c). The 3D pose estimation model achieved a MPJPE of 19.67 mm on the training dataset and 24.80 mm on the test dataset.

3.2. Accuracy of the angular biomarkers

The MAE and PCC for the individual biomarkers are shown in Table 3. The average MAE and PCC across all angular biomarkers were 2.3° and 0.75 respectively. All angular biomarkers had a MAE of less than 5.2°. 22 out of the 30 angular biomarkers had PCC greater than 0.7. Pelvic anterior tilt, knee varus, ankle inversion and ankle rotation had lower PCC. The accuracies of left and right biomarkers were similar.

The mean joint angles across the gait cycle computed by 3DGait and by OptiTrack were plotted along with the MAE in Fig. 4 (see Sup. Fig. S4

Table 2
Performance of the pose estimation models on the training and test data, and various 2D image datasets.

Model	2D pose estimation		3D pose estimation
Metric	OKS	Pixel error	MPJPE (mm)
Training	0.945	7.49	19.67
Test subjects in black body suit	0.889	10.29	24.80
Test subjects in everyday clothing	0.875	11.32	–
MS-COCO validation set[a]	0.835	13.16	–

[a] Evaluation was done on a subset of images in the MS-COCO validation set in which the whole body is visible.

Table 3
Accuracy of the angular joint kinematics.

No.	Biomarker name	MAE (95 % C.I.)		PCC (95 % C.I.)	
		Left	Right	Left	Right
1	Pelvic Anterior Tilt	0.65° (0.48–0.82)	0.66° (0.45–0.87)	0.63 (0.42–0.83)	0.55 (0.34–0.76)
2	Pelvic Up Obliquity	0.99° (0.72–1.25)	0.94° (0.66–1.22)	0.87 (0.79–0.95)	0.87 (0.81–0.94)
3	Pelvic Internal Rotation	1.08° (0.82–1.35)	1.10° (0.80–1.40)	0.89 (0.82–0.96)	0.88 (0.79–0.97)
4	Hip Flexion	2.80° (1.86–3.74)	2.83° (1.90–3.75)	0.98 (0.97–0.99)	0.98 (0.97–0.99)
5	Hip Adduction	1.17° (0.88–1.46)	1.22° (1.02–1.41)	0.88 (0.80–0.95)	0.88 (0.82–0.94)
6	Hip Internal Rotation	2.02° (1.64–2.39)	2.28° (1.81–2.75)	0.75 (0.64–0.86)	0.74 (0.59–0.90)
7	Knee Flexion	4.34° (2.73–5.94)	5.18° (3.65–6.71)	0.96 (0.93–1.00)	0.94 (0.90–0.99)
8	Knee Varus	2.73° (1.28–4.19)	2.38° (1.53–3.22)	0.05 (−0.53–0.63)	0.33 (0.02–0.64)
9	Knee Internal Rotation	2.79° (2.28–3.20)	2.56° (1.78–3.34)	0.86 (0.79–0.93)	0.85 (0.73–0.97)
10	Ankle Dorsiflexion	2.32° (1.56–3.08)	2.58° (1.83–3.34)	0.90 (0.83–0.97)	0.88 (0.80–0.95)
11	Ankle Inversion	2.89° (1.92–3.86)	3.87° (1.87–5.87)	0.60 (0.36–0.85)	0.40 (0.09–0.71)
12	Ankle Rotation	2.34° (1.46–3.02)	2.68° (1.96–3.41)	0.10 (−0.23–0.43)	0.20 (−0.11–0.51)
13	Foot Internal Progression	2.16° (1.74–2.58)	2.51° (1.74–3.27)	0.86 (0.75–0.97)	0.87 (0.78–0.97)
14	Elbow Flexion	2.51° (1.89–3.14)	2.03° (0.85–3.21)	0.92 (0.85–1.00)	0.93 (0.84–1.00)
15	Shoulder Flexion	2.62° (1.77–3.48)	2.90° (2.11–3.69)	0.97 (0.93–1.00)	0.95 (0.91–1.00)
	Mean	2.22° (1.87–2.57)	2.38° (2.12–2.65)	0.75 (0.71–0.79)	0.74 (0.70–0.78)

for individual data points). The MAE was less than 5° and had little variation across the gait cycle for most biomarkers except knee flexion and foot internal progression, which had higher errors during the later half of the gait cycle.

SPM1d analysis (Fig. 5) showed no significant difference between 3DGait and marker-based MoCap across the gait cycle for most joint angles. There was a significant difference during the transition to swing phase for hip and knee flexion, during the early stance phase for knee varus, and during the swing phase for shoulder flexion.

3.3. Accuracy of the spatiotemporal biomarkers

Table 4 shows the MAE between spatiotemporal biomarkers computed using 3DGait and ground truth marker-based MoCap. For temporal biomarkers (excluding TUG time), errors were below 0.03 s—equivalent to 1 frame in a 30 frames per second video. TUG had a higher MAE of 0.163 s, but this represents 1.23 % of the ground truth value. All spatiotemporal biomarkers showed MAE of less than 15 % relative to ground truth values.

4. Discussion

In this study, we introduced 3DGait, an innovative single-camera, markerless gait analysis system designed to enhance clinical and home-based monitoring. Evaluated against marker-based MoCap in 8 healthy adults, 3DGait demonstrated comparable accuracy while operating with a widely available mobile device. Our 2D pose model performed robustly across diverse subjects, clothing and environments (Table 2, Sup. Fig. S3). Performance was lower on the MS-COCO dataset, which was expected due to the inclusion of complex, non-test scenarios. The 3D pose model achieved a MPJPE of 24.8 mm, comparable to open-source methods (30–50 mm; (Needham et al., 2021) and Theia3D (25–36 mm; (Kanko et al., 2021a).

Angular biomarker showed an average MAE of 2.3° and a PCC of 0.75, with consistent performance across both body sides. Joint kinematics closely aligned with MoCap measurements, though errors tended to increase during rapid joint movements, particularly during transitions into and throughout the swing phase for knee, hip, and shoulder flexion (Figs. 4, 5). These errors likely stem from gait cycle misalignments, motion blur and 2D key point variability. Depth estimation limitations from a frontal view further impact sagittal plane angle accuracy. In contrast, knee varus discrepancies during stance phase likely result from its small range of motion, which is harder to detect with markerless systems.

Most angular biomarkers from 3DGait showed strong correlation (>0.7) with MoCap, except for pelvic anterior tilt and ankle inversion (moderate, 0.5–0.7) and ankle rotation and knee varus (poor, <0.5) (classification based on (Mukaka, 2012)). Moderate to low PCC biomarkers had small MAEs (0.65°–3.87°), likely due to their limited range of motion (<15°, Fig. 4) which makes PCC sensitive to small variations and a less reliable metric (Janse et al., 2021). Additionally, slight inaccuracies in pose estimation can disproportionately impact subtle joint movements (Colyer et al., 2018; D'Souza et al., 2024; Turner et al., 2024), due to depth perception issues, occlusions, and small angular displacements (Wade et al., 2022).

3DGait's angular biomarker accuracy is comparable to other markerless systems (Table 5) (Kanko et al., 2021a; Stenum et al., 2024; Turner et al., 2024) and outperforms Kinect-based approaches (Choppin et al., 2014; Guess et al., 2017; Springer and Seligmann, 2016). Its use of a depth sensor and specialized 3D pose estimation model enhanced out-of-plane joint kinematics accuracy—an area where many existing systems struggle (Scott et al., 2022; Springer and Seligmann, 2016).

All spatiotemporal biomarkers measured by 3DGait had errors below 15 %. Temporal parameters were particularly accurate, with errors equivalent to one frame in a 30 FPS video, consistent with other systems (Clark et al., 2013; Kanko et al., 2021b; McGuirk et al., 2022; Pfister

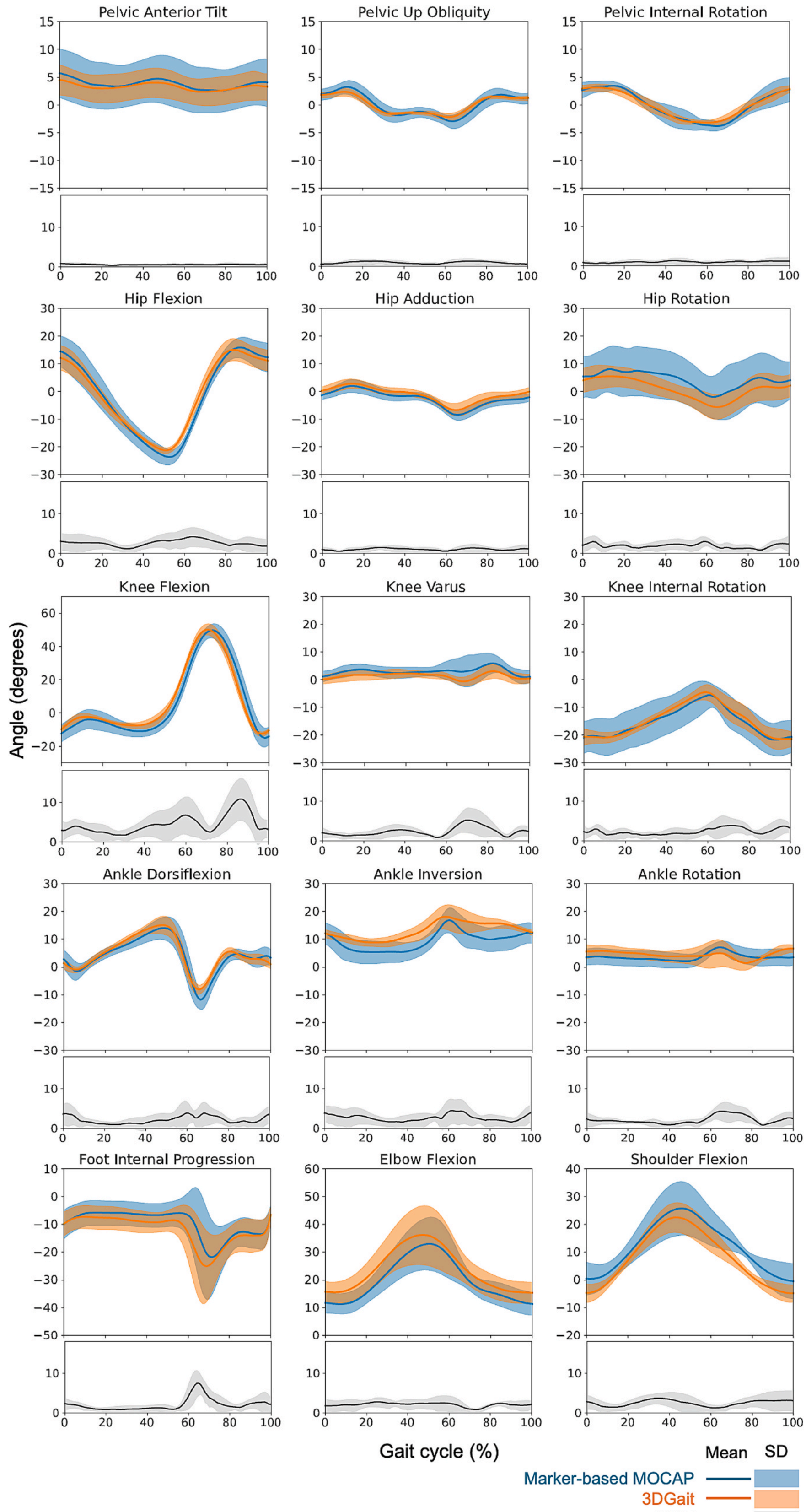

Fig. 4. Joint angles, averaged across left and right sides, during the gait cycle derived from the marker-based MoCap system (OptiTrack, blue) and from our single camera markerless system (3DGait, orange). Black line below each plot shows the mean-shifted MAE between the two systems. Solid line represents mean and shaded area represents standard deviation across the 8 subjects. (For interpretation of the references to color in this figure legend, the reader is referred to the web version of this article.)

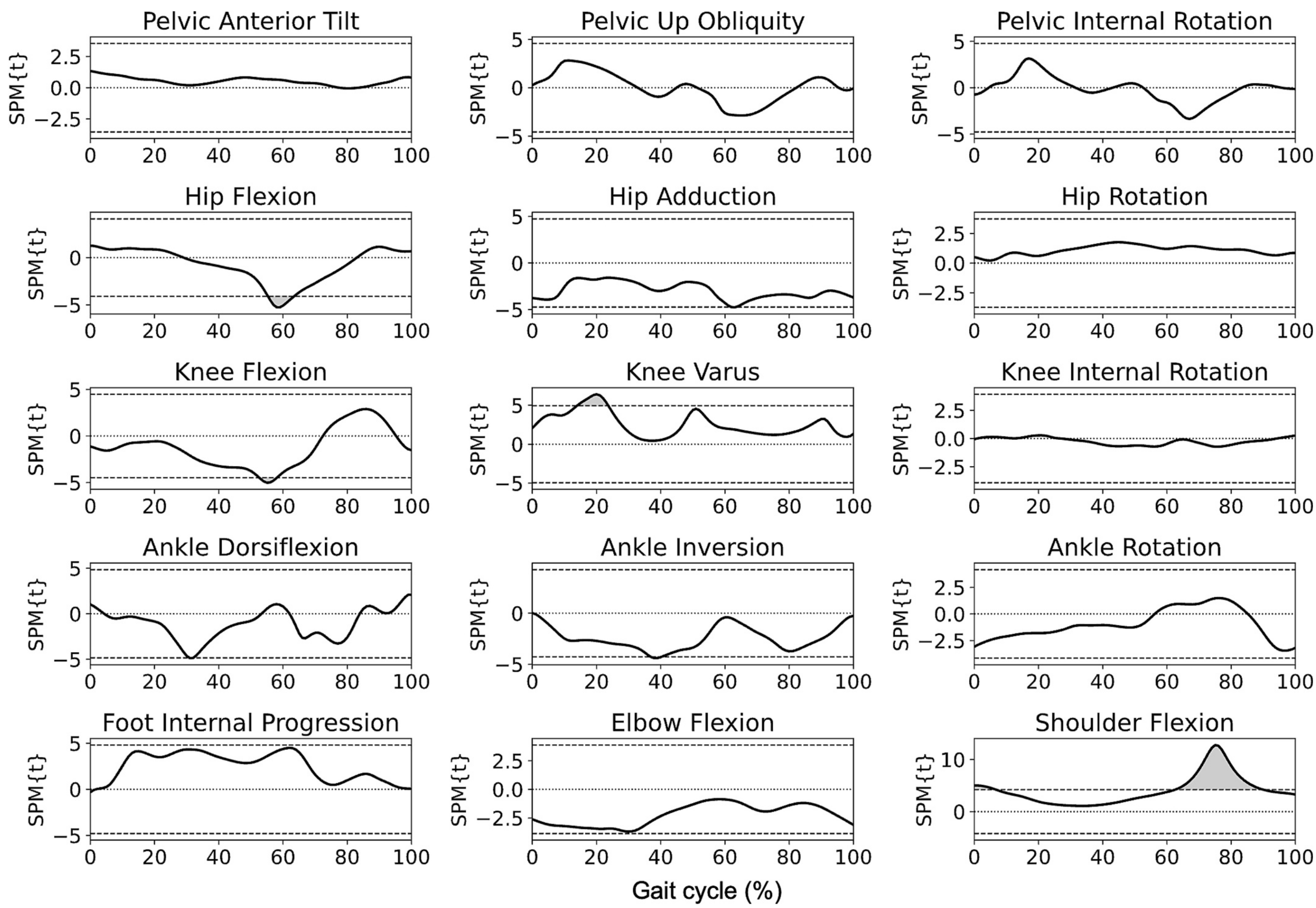

Fig. 5. Statistical Parametric Mapping (SPM1d) analysis of joint kinematics. SPM{t} statistical maps from paired t-tests comparing 3DGait and marker-based MoCap joint angle trajectories over a normalized gait cycle (0–100 %). The solid black lines represent the t-statistic across the gait cycle, and the horizontal dashed lines indicate the critical threshold for statistical significance at $p < 0.05$, determined using random field theory. Shaded regions (if present) denote significant differences between the two methods.

Table 4
Accuracy of the spatiotemporal gait parameters.

No.	Biomarker name	MAE (95 % C.I.)		MAE as % of ground truth (95 % C.I.)	
		Left	Right	Left	Right
1	Stride Length (m)	0.120 (0.080–0.161)	0.112 (0.086–0.138)	9.44 (6.37–12.52)	8.90 (6.94–10.86)
2	Stride Duration (s)	0.011 (0.006–0.016)	0.009 (0.003–0.015)	0.99 (0.56–1.42)	0.77 (0.22–1.33)
3	Stride Speed (m/s)	0.104 (0.076–0.132)	0.096 (0.082–0.109)	9.34 (6.63–12.05)	8.60 (7.22–9.99)
4	Step Length (m)	0.046 (0.030–0.061)	0.093 (0.070–0.117)	7.20 (4.85–9.56)	14.79 (11.23–18.34)
5	Step Duration (s)	0.014 (0.009–0.020)	0.018 (0.010–0.026)	2.50 (1.50–3.50)	3.17 (1.84–4.50)
6	Step Speed (m/s)	0.090 (0.056–0.124)	0.141 (0.097–0.185)	8.03 (5.03–11.02)	12.85 (8.59–17.10)
7	Gait Speed (m/s)	0.100 (0.083–0.114)		8.87 (7.28–10.47)	
8	Single Support (s)	0.018 (0.006–0.030)	0.008 (0.002–0.014)	4.94 (1.41–8.46)	2.03 (0.37–3.68)
9	Double Support (s)	0.018 (0.009–0.027)	0.016 (0.006–0.025)	10.48 (3.73–17.23)	8.63 (4.05–13.22)
10	Total Double Support (s)	0.025 (0.005–0.045)		7.04 (1.49–12.58)	
11	Timed Up and Go (TUG) Test Time (s)	0.163 (0.008–0.319)		1.23 (0.05–2.42)	

et al., 2014; Springer and Seligmann, 2016; Stenum et al., 2024, 2021). Spatial errors are higher, due to 3DGait's use of a single, flexibly placed camera rather than fixed or multi-camera setups—a deliberate trade-off that prioritizes usability over marginal gains in accuracy.

Although 3DGait's does not match the sub-millimeter precision of high-end marker-based MoCap systems, errors below 5° are generally acceptable for clinical gait assessments (McGinley et al., 2009). This makes 3DGait well-suited for routine clinical evaluations and home

Table 5
Comparison of 3DGait against other markerless solutions for gait analysis.

Feature	3DGait	Theia3D	OpenCap	Microsoft/Azure Kinect (discontinued)[b] + accompanying software	Single camera systems
Accuracy (Joint kinematics)	• MAE 2.3° • PCC 0.75	• RMSE < 5.5° (except axial rotations)	• MAE 3.85°, RMSE 4.34° • CMC > 0.84 (sagittal), 0.47–0.78 (frontal, transverse)	• RMSE 5-12° • PCC variable	• MAE < 5° (Stenum et al., 2024), <11° (Viswakumar et al., 2022) • PCC > 0.8 (Wang et al., 2024)
Accuracy (Spatiotemporal parameters)	• Overall < 15 % error • Temporal MAE < 0.03 s • Spatial MAE 0.046–0.120 *m* • Speed MAE 0.1 m/s	• Temporal MAE 0.01–0.07 s • Spatial MAE < 0.01 *m* • Speed MAE < 0.02 m/s	Unknown	• Temporal ~ 10–20 % error • Spatial ~ 5 % error • Spatiotemporal PCC 0.69–0.99;	• Temporal MAE 0.01–0.05 s • Spatial MAE 0.021–0.074 *m* • Gait speed MAE 0.03–0.15 m/s
Ease of use and setup	• Single iPad Pro • No calibration • Auto person of interest detection in multi-person scene • Intuitive UI with placement guide	• 6–8 high-speed camera • Calibration needed	• 2 + RGB cameras • Calibration needed • Requires internet	• Single RGB-D camera • No calibration needed • Depends on third-party software for gait analysis	• Single RGB camera • No calibration but known location required and fixed frontal/sagittal view • No turnkey app
Space requirements	Small space, flexible set up	Large space required for multiple cameras	Moderate space for 2 cameras placed 30-45° apart	Limited to small capture volume (1–2 m from sensor)	Small space for frontal view, large space for sagittal view
Cost	• Hardware: ~US $800–1200 (iPad Pro) • Software: Subscription based	• Hardware: ~US$25 k (cameras) + US$5–8 k (GPU) • Software: Subscription and lifetime license	• Hardware: US$1–3 k (2 cameras) • Software: free but paid version available for coaches / clinicians	• Hardware: ~US$150–400 (Kinect) + US$5–8 k (GPU) • Software: Official SDK is free, third-party applications may have additional fees	• Hardware: <US$500 (camera) + US$5–8 k (GPU) • Software: free
Analysis time	~1 min for a 15 s video (0.14 s per frame) [a]	0.005 – 0.15 s per frame, depending on computing power	~5 min per trial	Several minutes per trial, depending on computing power	0.1–0.2 s per frame
Privacy and data security	• All processing done locally on iPad • Automatic face-blurring • Immediate video deletion option	• Local GPU processing • No built-in privacy features	• Cloud processing • No built-in privacy features	• Local GPU processing • No built-in privacy features	• Local GPU processing • No built-in privacy features
Main use cases	Broad clinical, rehabilitation and home use	Clinical gait analysis, research, advanced sports science	Research, education, exploratory clinical use	Research, consumer and home use	Research prototypes
References		D'Souza et al., 2024; Kanko et al., 2021a, 2021b; Wren et al., 2023; McGuirk et al., 2022	Turner et al., 2024; Uhlrich et al., 2023	Choppin et al., 2014;Clark et al., 2013;Guess et al., 2017; Pfister et al., 2014;Springer & Seligmann, 2016	Stenum et al., 2021, 2024; Viswakumar et al., 2022; Wang et al., 2024

MAE = Mean Absolute Error, RMSE = Root Mean Squared Error, CMC = Coefficient of Multiple Correlation, PCC = Pearson's Correlation Coefficient.
[a] We measured the average time taken for the full analysis to be done on the 16 test trials using an iPad Pro 11-ich (M4). The average time per frame is based on the total time divided by the number of frames in the video.
[b] Microsoft Kinect (Kinect for Windows) and Azure Kinect DK have been discontinued.

monitoring, where usability and portability are prioritized over high precision. For applications requiring higher accuracy, such as post-surgical rehabilitation monitoring, integrating additional sensors like IMUs (Petraglia et al., 2019) and future model enhancements may provide the needed improvements.

Future work will refine the pose estimation models by using biomechanical priors such as joint range limits and inter-joint coupling, integrating detailed lower-body parametric models, adopting depth-aware learning to better localize occluded joints, and expanding the training dataset with examples exhibiting subtle gait features. These enhancements should boost accuracy for angular biomarkers with small or complex movements, improve depth-informed spatial parameters and strengthen 3DGait's overall robustness.

The major advantage of 3DGait is its clinical accessibility (Table 5). It operates locally on a single iPad Pro—no high-end GPUs, cloud computing, multi-camera setups or calibration required. It features an intuitive, end-to-end interface and automatically generates clinically relevant gait parameters within 1–2 min, removing the need for biomechanics expertise or manual analysis. 3DGait automatically detects the target individual in multi-person environments, which is particularly useful in busy clinical settings. It also functions effectively in small, flexible spaces, unlike systems that require fixed camera orientations (Stenum et al., 2021, 2024) or large capture environments.

Cost-wise, 3DGait is more affordable than many markerless systems, requiring only an iPad Pro for hardware, though it operates on a subscription-based software model. Unlike other systems, privacy and data security are built in—all video processing occurs locally, faces are automatically blurred, and users can delete videos immediately—ensuring compliance with healthcare data privacy standards.

Deploying 3DGait in real-world conditions presents challenges such as varying lighting, clothing, and camera placement. Our 2D model was trained with diverse lighting, attire, and camera angles, while our 3D model incorporated different subject positions and camera views. A user-friendly interface also provides real-time guidance on optimal setup to support consistent data collection (Sup. Fig. S1). Still, further validation against validated markerless multi-camera systems or IMUs is essential to rigorously assess 3DGait's accuracy across varied real-world conditions, including different clothing types and fits, lighting environments, and camera configurations. Until then, results obtained under unvalidated conditions should be interpreted with caution.

Our test sample included 8 healthy adults of Chinese ethnicity, balanced for gender and age, drawn from a 72-subject dataset. Although external datasets (e.g. MS-COCO) were used to diversify training, the limited size and lack of ethnic diversity in the test set severely constrains generalizability. It is crucial to validate 3DGait on larger and more diverse populations, including individuals of various ethnicities, age groups—particularly middle-aged adults (30–50 years), where early gait changes may occur—and those with gait abnormalities.

Preliminary results suggested that 3DGait can detect reduced gait speed, shorter step length and increased stride variability in pre–frail and frail cardiac patients (Koh et al., 2025). A post-stroke validation study is also underway and will be reported separately. Future studies will extend validation to additional clinical populations (e.g. Parkinson's disease) and multi-site trials to assess robustness in real-world clinical environments. Longitudinal investigations will also be critical to evaluate 3DGait's ability to track gait changes over time for rehabilitation and chronic disease management.

Currently, 3DGait is limited to assessing walking and the TUG test, which are well established in clinical settings, especially for rehabilitation and frailty assessments (Harada et al., 1999; Herman et al., 2010; Mehdipour et al., 2024; Podsiadlo and Richardson, 1991). They were chosen to address the primary objective of evaluating gait and everyday functional mobility, but do not capture the full range of movements observed in clinical practice. Future work will incorporate more comprehensive functional assessments, including treadmill running, Short Physical Performance Battery (SPPB) (Guralnik et al., 1994) and Berg Balance Scale (Berg, 1989), to evaluate running, balance, coordination, and transitional movements more thoroughly.

The current system supports only a single frontal camera view, which is well suited for compact spaces like outpatient clinics but limits versatility and restricts the analysis of out-of-plane motion. Future versions will support alternative camera views and tasks involving lateral movement, turning, and dynamic balance challenges to expand clinical applicability.

Lastly, 3DGait currently outputs fixed biomarkers using predefined body segment and joint angle models. While this simplifies use, it limits custom analysis and data export. Future updates may enable customizable outputs to support more advanced research, while preserving ease of use for clinical applications.

5. Conclusion

3DGait is a clinically feasible, scalable, and accessible markerless gait analysis system that delivers accuracy comparable to marker-based MoCap without requiring multi-camera setups. Its single-camera, depth-integrated design enables seamless use in clinical, rehabilitation, and home settings with minimal setup. By operating on widely available consumer devices and performing real-time on-device processing, 3DGait supports routine assessments, fall risk screening, chronic disease management, and rehabilitation, even in resource-limited settings. Further validation in diverse populations and environments will strengthen its clinical impact, positioning 3DGait as a versatile and practical tool for gait assessment, remote monitoring and rehabilitation in modern healthcare.

CRediT authorship contribution statement

Ling Guo: Writing – review & editing, Writing – original draft, Software, Methodology, Formal analysis, Data curation. **Richard Chang:** Writing – review & editing, Software, Methodology, Formal analysis. **Jie Wang:** Writing – review & editing, Software, Methodology, Formal analysis. **Amudha Narayanan:** Writing – review & editing, Software, Methodology, Formal analysis. **Peisheng Qian:** Writing – review & editing, Software, Methodology. **Mei Chee Leong:** Writing – review & editing, Software, Methodology. **Partha Pratim Kundu:** Writing – review & editing, Writing – original draft, Software, Methodology, Formal analysis. **Sriram Senthilkumar:** Writing – review & editing, Software, Methodology, Formal analysis. **Sai Chaitanya Garlapati:** Writing – review & editing, Formal analysis. **Elson Ching Kiat Yong:** Writing – review & editing, Project administration, Funding acquisition, Conceptualization. **Ramanpreet Singh Pahwa:** Writing – review & editing, Writing – original draft, Supervision, Software, Project administration, Methodology, Funding acquisition, Conceptualization.

Declaration of competing interest

The authors declare the following financial interests/personal relationships which may be considered as potential competing interests: [3DGait is a commercial tool developed for sale and distribution. This research received partial funding from Carecam Pte. Ltd., a for-profit company that owns and developed the 3DGait system. Authors L. G., J. W., P. P. K., E. C. K. Y., S. S., S.C.P. and R. S. P. are current or former employees of Carecam Pte. Ltd. and contributed to the research, development, and evaluation of 3DGait. Additionally, authors E. C. K. Y. and R. S. P. hold shares or stock options in Carecam Pte. Ltd. Other authors have no conflict of interest to declare. The data collection, analysis, interpretation, and manuscript drafting were conducted objectively by the researchers without commercial interference. Carecam Pte Ltd. did not influence or control any aspect of the study's methodological design, data collection, analysis processes, interpretation of the results, or writing of the manuscript].

Acknowledgements

This research is partially supported by Innovation and Enterprise Office (IEO) Decentralised GAP (Grant No. I23D1AG090) which is supported and administered by the Agency for Science, Technology and Research (A*STAR), Singapore.

We thank Dr. Lisa MacFadden for her advice and feedback on this research and manuscript.

Appendix A. Sup. data

Sup. data to this article can be found online at https://doi.org/10.1016/j.jbiomech.2025.112738.

References

Aurand, A.M., Dufour, J.S., Marras, W.S., 2017. Accuracy map of an optical motion capture system with 42 or 21 cameras in a large measurement volume. J Biomech 58, 237–240. https://doi.org/10.1016/J.JBIOMECH.2017.05.006.

Berg, K., 1989. Measuring balance in the elderly: preliminary development of an instrument. Physiotherapy Canada 41, 304–311. https://doi.org/10.3138/ptc.41.6.304.

Boldo, M., Di Marco, R., Martini, E., Nardon, M., Bertucco, M., Bombieri, N., 2024. On the reliability of single-camera markerless systems for overground gait monitoring. Comput Biol Med 171. https://doi.org/10.1016/j.compbiomed.2024.108101.

Cao, Z., Simon, T., Wei, S.E., Sheikh, Y., 2017. Realtime multi-person 2d pose estimation using part affinity fields. In: In: Proceedings of the IEEE Conference on Computer Vision and Pattern Recognition, pp. 7291–7299.

Cappozzo, A., Catani, F., Della Croce, U., Leardini, A., 1995. Position and orientation in space of bones during movement: anatomical frame definition and determination. Clinical Biomechanics 10, 171–178. https://doi.org/10.1016/0268-0033(95)91394-T.

Choppin, S., Lane, B., Wheat, J., 2014. The accuracy of the Microsoft Kinect in joint angle measurement. Sports Technology 7, 98–105. https://doi.org/10.1080/19346182.2014.968165.

Clark, R.A., Bower, K.J., Mentiplay, B.F., Paterson, K., Pua, Y.H., 2013. Concurrent validity of the Microsoft Kinect for assessment of spatiotemporal gait variables. J Biomech 46, 2722–2725. https://doi.org/10.1016/j.jbiomech.2013.08.011.

Colyer, S.L., Evans, M., Cosker, D.P., Salo, A.I.T., 2018. A Review of the Evolution of Vision-Based Motion Analysis and the Integration of Advanced Computer Vision Methods Towards Developing a Markerless System. Sports Med Open 4, 1–15. https://doi.org/10.1186/S40798-018-0139-Y/FIGURES/4.

Corazza, S., Mündermann, L., Chaudhari, A.M., Demattio, T., Cobelli, C., Andriacchi, T. P., 2006. A markerless motion capture system to study musculoskeletal

biomechanics: Visual hull and simulated annealing approach. Ann Biomed Eng 34, 1019–1029. https://doi.org/10.1007/s10439-006-9122-8.
Dogan, S., Shi, X., Dawes, H., Bradbury, K., Weightman, A., Cooper, G., Sanders, O., Wang, B., Kontson, K., 2024. Concurrent Validity Evidence for Pressure-Sensing Walkways Measuring Spatiotemporal Features of Gait: A Systematic Review and Meta-Analysis. Sensors 2024, Vol. 24, Page 4537 24, 4537. doi: 10.3390/S24144537.
Drazan, J.F., Phillips, W.T., Seethapathi, N., Hullfish, T.J., Baxter, J.R., 2021. Moving outside the lab: Markerless motion capture accurately quantifies sagittal plane kinematics during the vertical jump. J Biomech 125. https://doi.org/10.1016/j.jbiomech.2021.110547.
D'Souza, S., Siebert, T., Fohanno, V., 2024. A comparison of lower body gait kinematics and kinetics between Theia3D markerless and marker-based models in healthy subjects and clinical patients. Sci Rep 14, 29154. https://doi.org/10.1038/s41598-024-80499-8.
Ehara, Y., Fujimoto, H., Miyazaki, S., Mochimaru, M., Tanaka, S., Yamamotoe, S., 1997. Comparison of the performance of 3D camera systems II. Gait Posture 5, 251–255.
Ehara, Y., Fujimoto, H., Miyazaki, S., Tanaka, S., Yamamoto, S., 1995. Comparison of the performance of 3D camera systems. Gait Posture 3, 166–169. https://doi.org/10.1016/0966-6362(95)99067-U.
Fischler, M.A., Bolles, R.C., 1981. Random sample consensus: a paradigm for model fitting with applications to image analysis and automated cartography. Commun ACM 24, 381–395. https://doi.org/10.1145/358669.358692.
Grood, E.S., Suntay, W.J., 1983. A Joint Coordinate System for the Clinical Description of Three-Dimensional Motions. Application to the Knee.
Guess, T.M., Razu, S., Jahandar, A., Skubic, M., Huo, Z., 2017. Comparison of 3D Joint Angles Measured With the Kinect 2.0 Skeletal Tracker Versus a Marker-Based Motion Capture System. J Appl Biomech 33, 176–181. https://doi.org/10.1123/JAB.2016-0107.
Guralnik, J.M., Simonsick, E.M., Ferrucci, L., Glynn, R.J., Berkman, L.F., Blazer, D.G., Scherr, P.A., Wallace, R.B., 1994. A Short Physical Performance Battery Assessing Lower Extremity Function: Association With Self-Reported Disability and Prediction of Mortality and Nursing Home Admission. J Gerontol 49, M85–M94. https://doi.org/10.1093/GERONJ/49.2.M85.
Harada, N.D., Chiu, V., Stewart, A.L., 1999. Mobility-related function in older adults: Assessment with a 6-minute walk test. Arch Phys Med Rehabil 80, 837–841. https://doi.org/10.1016/S0003-9993(99)90236-8.
Herman, T., Giladi, N., Hausdorff, J.M., 2010. Properties of the 'Timed Up and Go' Test: More than Meets the Eye. Gerontology 57, 203. https://doi.org/10.1159/000314963.
Homan, K., Yamamoto, K., Kadoya, K., Ishida, N., Iwasaki, N., 2022. Comprehensive validation of a wearable foot sensor system for estimating spatiotemporal gait parameters by simultaneous three-dimensional optical motion analysis. BMC Sports Sci Med Rehabil 14, 1–11. https://doi.org/10.1186/S13102-022-00461-X/FIGURES/4.
Hulleck, A.A., Menoth Mohan, D., Abdallah, N., El Rich, M., Khalaf, K., 2022. Present and future of gait assessment in clinical practice: Towards the application of novel trends and technologies. Front Med Technol 4. https://doi.org/10.3389/FMEDT.2022.901331.
Janse, R.J., Hoekstra, T., Jager, K.J., Zoccali, C., Tripepi, G., Dekker, F.W., Van Diepen, M., 2021. Conducting correlation analysis: important limitations and pitfalls. Clin Kidney J 14, 2332–2337. https://doi.org/10.1093/CKJ/SFAB085.
Kanko, R.M., Laende, E.K., Davis, E.M., Selbie, W.S., Deluzio, K.J., 2021a. Concurrent assessment of gait kinematics using marker-based and markerless motion capture. J Biomech 127. https://doi.org/10.1016/j.jbiomech.2021.110665.
Kanko, R.M., Laende, E.K., Strutzenberger, G., Brown, M., Selbie, W.S., DePaul, V., Scott, S.H., Deluzio, K.J., 2021b. Assessment of spatiotemporal gait parameters using a deep learning algorithm-based markerless motion capture system. J Biomech 122. https://doi.org/10.1016/j.jbiomech.2021.110414.
Koh, A.-S.-M., Benjamin, L.J.J., Loh, J., Pahwa, R.S., Chang, R., Wang, J., Meng, B., Si Lin, L., Lee, G., Ng, H.J., Teo, L.Y., 2025. A Real-time Artificial Intelligence-Based Gait Analysis Tool Identifies Gait Characteristics Associated with Pre-frailty and Cardiac Frail Patients. J Am Coll Cardiol 85, 2540. https://doi.org/10.1016/S0735-1097(25)03024-4.
Lam, W.W.T., Tang, Y.M., Fong, K.N.K., 2023. A systematic review of the applications of markerless motion capture (MMC) technology for clinical measurement in rehabilitation. J Neuroeng Rehabil 20, 1–26. https://doi.org/10.1186/S12984-023-01186-9/TABLES/2.
Lin, T.-Y., Maire, M., Belongie, S., Hays, J., Perona, P., Ramanan, D., Dollár, P., Zitnick, L. C., 2014. Microsoft coco: Common objects in context, in: Computer Vision–ECCV 2014: 13th European Conference, Zurich, Switzerland, September 6-12, 2014, Proceedings, Part V 13,. Springer International Publishing, pp. 740–755.
Liu, X., Zhao, C., Zheng, B., Guo, Q., Duan, X., Wulamu, A., Zhang, D., 2021. Wearable Devices for Gait Analysis in Intelligent Healthcare. Front Comput Sci 3, 661676. https://doi.org/10.3389/FCOMP.2021.661676/BIBTEX.
Maji, D., Nagori, S., Mathew, M., Poddar, D., 2022. Yolo-pose: Enhancing yolo for multi person pose estimation using object keypoint similarity loss. In: In: Proceedings of the IEEE/CVF Conference on Computer Vision and Pattern Recognition, pp. 2637–2646.
Mathis, A., Schneider, S., Lauer, J., Mathis, M.W., 2020. A Primer on Motion Capture with Deep Learning: Principles, Pitfalls, and Perspectives. Neuron 108, 44–65. https://doi.org/10.1016/J.NEURON.2020.09.017/ATTACHMENT/46E265F6-9FF2-4F64-9116-B8CC9C958FC4/MMC1.MP4.
McGinley, J.L., Baker, R., Wolfe, R., Morris, M.E., 2009. The reliability of three-dimensional kinematic gait measurements: A systematic review. Gait Posture. https://doi.org/10.1016/j.gaitpost.2008.09.003.
McGuirk, T.E., Perry, E.S., Sihanath, W.B., Riazati, S., Patten, C., 2022. Feasibility of Markerless Motion Capture for Three-Dimensional Gait Assessment in Community Settings. Front Hum Neurosci 16, 867485. https://doi.org/10.3389/FNHUM.2022.867485/BIBTEX.
Mehdipour, A., Malouka, S., Beauchamp, M., Richardson, J., Kuspinar, A., 2024. Measurement properties of the usual and fast gait speed tests in community-dwelling older adults: a COSMIN-based systematic review. Age Ageing 53, afae055. https://doi.org/10.1093/AGEING/AFAE055.
Moro, M., Marchesi, G., Hesse, F., Odone, F., Casadio, M., 2022. Markerless vs. Marker-Based Gait Analysis: A Proof of Concept Study. Sensors 2022, Vol. 22, Page 2011 22, 2011. doi: 10.3390/S22052011.
Mukaka, M.M., 2012. A guide to appropriate use of Correlation coefficient in medical research. Malawi Med J 24, 69.
Mündermann, L., Corazza, S., Andriacchi, T.P., 2006. The evolution of methods for the capture of human movement leading to markerless motion capture for biomechanical applications. J Neuroeng Rehabil 3, 1–11. https://doi.org/10.1186/1743-0003-3-6/FIGURES/5.
Muro-de-la-Herran, A., García-Zapirain, B., Méndez-Zorrilla, A., 2014. Gait Analysis Methods: An Overview of Wearable and Non-Wearable Systems, Highlighting Clinical Applications. Sensors 2014, Vol. 14, Pages 3362-3394 14, 3362–3394. doi: 10.3390/S140203362.
Needham, L., Evans, M., Cosker, D.P., Wade, L., McGuigan, P.M., Bilzon, J.L., Colyer, S. L., 2021. The accuracy of several pose estimation methods for 3D joint centre localisation. Scientific Reports 2021 11:1 11, 1–11. doi: 10.1038/s41598-021-00212-x.
Pavllo, D., Feichtenhofer, C., Grangier, D., Auli, M., 2019. 3D human pose estimation in video with temporal convolutions and semi-supervised training. In: In: Proceedings of the IEEE/CVF Conference on Computer Vision and Pattern Recognition, pp. 7753–7762.
Petraglia, F., Scarcella, L., Pedrazzi, G., Brancato, L., Puers, R., Costantino, C., 2019. Inertial sensors versus standard systems in gait analysis: A systematic review and meta-analysis. Eur J Phys Rehabil Med. https://doi.org/10.23736/S1973-9087.18.05306-6.
Pfister, A., West, A.M., Bronner, S., Noah, J.A., 2014. Comparative abilities of Microsoft Kinect and Vicon 3D motion capture for gait analysis. J Med Eng Technol 38, 274–280. https://doi.org/10.3109/03091902.2014.909540.
Podsiadlo, D., Richardson, S., 1991. The Timed "Up & Go": A Test of Basic Functional Mobility for Frail Elderly Persons. J Am Geriatr Soc 39, 142–148. https://doi.org/10.1111/J.1532-5415.1991.TB01616.X.
Richards, J.G., 1999. The measurement of human motion: A comparison of commercially available systems. Hum Mov Sci 18, 589–602. https://doi.org/10.1016/S0167-9457(99)00023-8.
Saboor, A., Kask, T., Kuusik, A., Alam, M.M., Le Moullec, Y., Niazi, I.K., Zoha, A., Ahmad, R., 2020. Latest research trends in gait analysis using wearable sensors and machine learning: A systematic review. IEEE Access 8, 167830–167864. https://doi.org/10.1109/ACCESS.2020.3022818.
Scataglini, S., Abts, E., Van Bocxlaer, C., Van den Bussche, M., Meletani, S., Truijen, S., 2024. Accuracy, Validity, and Reliability of Markerless Camera-Based 3D Motion Capture Systems versus Marker-Based 3D Motion Capture Systems in Gait Analysis: A Systematic Review and Meta-Analysis. Sensors 2024, Vol. 24, Page 3686 24, 3686. doi: 10.3390/S24113686.
Scott, B., Seyres, M., Philp, F., Chadwick, E.K., Blana, D., 2022. Healthcare applications of single camera markerless motion capture: a scoping review. PeerJ 10, e13517. https://doi.org/10.7717/PEERJ.13517/SUPP-1.
Simon, S.R., 2004. Quantification of human motion: Gait analysis - Benefits and limitations to its application to clinical problems. J Biomech 37, 1869–1880. https://doi.org/10.1016/j.jbiomech.2004.02.047.
Springer, S., Seligmann, G.Y., 2016. Validity of the Kinect for Gait Assessment: A Focused Review. Sensors 2016, Vol. 16, Page 194 16, 194. doi: 10.3390/S16020194.
Stenum, J., Hsu, M.M., Pantelyat, A.Y., Roemmich, R.T., 2024. Clinical gait analysis using video-based pose estimation: Multiple perspectives, clinical populations, and measuring change. PLOS Digital Health 3, e0000467. https://doi.org/10.1371/journal.pdig.0000467.
Stenum, J., Rossi, C., Roemmich, R.T., 2021. Two-dimensional video-based analysis of human gait using pose estimation. PLoS Comput Biol 17, e1008935. https://doi.org/10.1371/JOURNAL.PCBI.1008935.
Sun, K., Xiao, B., Liu, D., Wang, J., 2019. Deep high-resolution representation learning for human pose estimation, in. In: Proceedings of the IEEE/CVF Conference on Computer Vision and Pattern Recognition, pp. 5693–5703.
Tadano, S., Takeda, R., Miyagawa, H., 2013. Three Dimensional Gait Analysis Using Wearable Acceleration and Gyro Sensors Based on Quaternion Calculations. Sensors 2013, Vol. 13, Pages 9321-9343 13, 9321–9343. doi: 10.3390/S130709321.
Turner, J.A., Chaaban, C.R., Padua, D.A., 2024. Validation of OpenCap: A low-cost markerless motion capture system for lower-extremity kinematics during return-to-sport tasks. J Biomech 171, 112200. https://doi.org/10.1016/J.JBIOMECH.2024.112200.
Uhlrich, S.D., Falisse, A., Kidziński, Ł., Muccini, J., Ko, M., Chaudhari, A.S., Hicks, J.L., Delp, S.L., 2023. OpenCap: Human movement dynamics from smartphone videos. PLoS Comput Biol 19. https://doi.org/10.1371/journal.pcbi.1011462.
Viswakumar, A., Rajagopalan, V., Ray, T., Gottipati, P., Parimi, C., 2022. Development of a Robust, Simple, and Affordable Human Gait Analysis System Using Bottom-Up Pose Estimation With a Smartphone Camera. Front Physiol 12, 784865. https://doi.org/10.3389/FPHYS.2021.784865/BIBTEX.
Wade, L., Needham, L., McGuigan, P., Bilzon, J., 2022. Applications and limitations of current markerless motion capture methods for clinical gait biomechanics. PeerJ 10, e12995. https://doi.org/10.7717/PEERJ.12995/FIG-5.

Wang, C.-Y., Bochkovskiy, A., Liao, H.-Y.M., 2023. YOLOv7: Trainable bag-of-freebies sets new state-of-the-art for real-time object detectors, in: Proceedings of the IEEE/CVF Conference on Computer Vision and Pattern Recognition. pp. 7646–7475.

Wang, H., Su, B., Lu, L., Jung, S., Qing, L., Xie, Z., Xu, X., 2024. Markerless gait analysis through a single camera and computer vision. J Biomech 165, 112027. https://doi.org/10.1016/J.JBIOMECH.2024.112027.

Webster, K.E., Wittwer, J.E., Feller, J.A., 2005. Validity of the GAITRite® walkway system for the measurement of averaged and individual step parameters of gait. Gait Posture 22, 317–321. https://doi.org/10.1016/J.GAITPOST.2004.10.005.

Whittle, M.W., 2014. Gait analysis: an introduction. Butterworth-Heinemann.

Winter, D.A., 2009. Biomechanics and motor control of human movement. John Wiley & Sons.

Wojke, N., Bewley, A., Paulus, D., 2017. Simple online and realtime tracking with a deep association metric. IEEE, pp. 3645–3649.

Wren, T.A.L., Isakov, P., Rethlefsen, S.A., 2023. Comparison of kinematics between Theia markerless and conventional marker-based gait analysis in clinical patients. Gait Posture 104, 9–14. https://doi.org/10.1016/j.gaitpost.2023.05.029.

Xiao, B., Wu, H., Wei, Y., 2018. Simple baselines for human pose estimation and tracking, in. In: Proceedings of the European Conference on Computer Vision (ECCV), pp. 466–481.

Zhang, Z., Tang, J., Wu, G., 2019. Simple and Lightweight Human Pose Estimation.